

*Physics*

*Physics Research Publications*

---

*Purdue University*

*Year 2003*

---

Measurements of absorption coefficient  
and refractive index changes without the  
Kramers-Kronig relation in  
photorefractive quantum wells of GaAs

R. Ramos-Garcia

R. Chiu-Zarate

D. Nolte

M. R. Melloch

This paper is posted at Purdue e-Pubs.  
[http://docs.lib.purdue.edu/physics\\_articles/421](http://docs.lib.purdue.edu/physics_articles/421)

# Measurements of absorption coefficient and refractive index changes without the Kramers–Kronig relation in photorefractive quantum wells of GaAs

R Ramos-Garcia<sup>1</sup>, R Chiu-Zarate<sup>1</sup>, D Nolte<sup>2</sup> and M R Melloch<sup>3</sup>

<sup>1</sup> Instituto Nacional de Astrofísica, Óptica y Electrónica, Apartado Postal 51 y 216, Puebla Pue, Mexico

<sup>2</sup> Department of Physics, Purdue University, West Lafayette, IN 47907-1396, USA

<sup>3</sup> School of Electrical Engineering, Purdue University, West Lafayette, IN 47907-1396, USA

E-mail: rgarcia@inaoep.mx

Received 24 April 2003, accepted for publication 21 July 2003

Published 27 October 2003

Online at [stacks.iop.org/JOptA/5/S514](http://stacks.iop.org/JOptA/5/S514)

## Abstract

We measure the absorption coefficient and refractive index changes produced in photorefractive quantum wells of GaAs by using a high-sensitivity periodically phase-modulated two-wave mixing technique. The technique allows us to measure both the amplitude and phase of the refractive and absorption index changes simultaneously. Thus, there is no necessity to use the Kramers–Kronig relation when either the absorption or refractive index is known. We also measure the response time of the grating formation in the frequency domain, yielding  $\sim 15 \mu\text{s}$  at  $I_0 = 11 \text{ mW cm}^{-2}$ , which shows that quantum wells of GaAs are one of the fastest materials for dynamic holography.

**Keywords:** Quantum wells, photorefractivity, dynamic holography, nonlinear optics

## 1. Introduction

In photorefractive multiple quantum wells (PRMQW) [1] operating in the transverse configuration, measurements of the differential transmission spectra of a homogeneous beam with and without an applied field are typically used to evaluate the changes in the absorption coefficient (electroabsorption) associated with lifetime broadening of the transition lineshape of quantum-confined excitons [2]. The associated refractive index changes (electrorefraction) are usually calculated from the electroabsorption measurements by using the Kramers–Kronig relation. Thus, the total diffraction efficiency due to absorption and phase gratings can be calculated without actually writing any grating [3]. Another common way of measuring electroabsorption and electrorefraction in quantum well structures is from two-wave mixing (TWM) gain measurements. Interference of a pair of coherent plane-wave beams in PRMQW leads to periodically spatial modulation of the space-charge field. This space-charge field

broadens the lifetime of quantum-confined excitons spatially and thus absorption and refractive index gratings are written in PRMQW. Due to the symmetry properties of the absorption and refractive index gratings with respect to the applied electric field, it is possible to single out both components without requiring the Kramers–Kronig relation [4]. However, in trap-dominated materials such as semi-insulating GaAs, the trapping of charge leads to large electric field overshoots near the injecting contact, creating local fields that can be orders of magnitude from the applied field distribution alone [5]. Additionally, the final field distribution gives different values for negative or positive applied voltage. Thus, in order to apply TWM for electroabsorption and electrorefraction special care must be taken in order to deposit non-charge-blocking electrodes.

Here we describe a periodically phase-modulated two-wave mixing (PMTWM) technique to obtain simultaneously the absorption and refractive index contributions to the diffraction efficiency by using current contact technology.

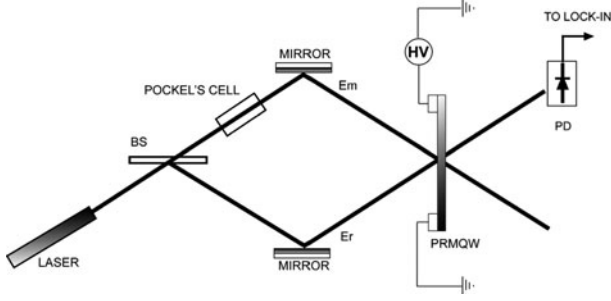


**Figure 1.** Interference between a periodically phase modulated ( $E_m$ ) and reference ( $E_r$ ) beam on the sample creates absorption and refractive index gratings when an external electric field is applied. Diffraction from the gratings generates a signal at  $\Omega$  and another at  $2\Omega$ , which are detected by a photodetector connected to a lock-in amplifier.

The technique allows us to measure both the amplitude and phase of the refractive and absorption index changes, and therefore their relative contributions to the diffraction efficiency. The advantage of this technique is that there is no need to use the Kramers–Kronig relation or to reverse the polarity of the applied field, as in [4], which is not always possible or easy to perform.

## 2. Phase-modulated holography

Figure 1 shows the schematic set-up used to measure simultaneously the absorption and refractive index grating. One arm of the interferometer is phase-modulated at the frequency  $\Omega$  by either a phase modulator or a mirror mounted on a piezoelectric crystal. The diffracted reference beam is detected by a photodetector connected to a lock-in amplifier. The diffracted reading beam amplitude can be written as

$$E_d = H E_r, \quad (1)$$

where  $E_r$  is the amplitude of the reading beam,  $E_d$  is the diffracted beam amplitude and  $H$  is the complex holographic diffraction amplitude, which for small diffraction amplitude ( $H \ll 1$ , typical of photorefractive quantum wells) can be written as

$$H = D \left( \frac{\Delta \alpha l}{4 \cos \theta} + i \frac{\pi \Delta n l}{\lambda \cos \theta} \right) \quad (2)$$

where  $D = \exp(-\alpha_0 l / \cos \theta)$  accounts for the attenuation of both beams due to the absorption  $\alpha_0$  of the quantum wells of thickness  $l$ ,  $\theta$  is the semi-angle between interfering beams,  $\Delta \alpha$  is the amplitude of the absorption grating,  $\Delta n$  is the amplitude of the refractive index grating and  $\lambda$  is the wavelength of both beams. In the photorefractive literature for quantum wells it is common to report the measurements of the output diffraction efficiency, in which case  $D = 1$ . The  $\pi/2$  phase difference (as indicated for the imaginary part of equation (2)) between the absorption and refractive index grating is crucial to separate and simultaneously measure both contributions, as we will show below.

Interference between a weakly phase-modulated beam  $E_m$  ( $\Delta \ll 1$ , where  $\Delta$  is the amplitude of the phase modulation) at the frequency  $\Omega$  and the reference beam  $E_r$  will produce a DC signal (neglected in this work), a synchronous homodyne

signal (proportional to the refractive index grating) and a signal oscillating at twice the modulation frequency (proportional to the absorption grating), the last two terms being given by [6]

$$S(\Omega) = -2\Delta D^2 E_m E_r \left( \frac{\pi \Delta n l}{\lambda \cos \theta} \right) \sin \Omega t \quad (3)$$

$$S(2\Omega) = -\frac{1}{2} \Delta^2 D^2 E_m E_r \left( \frac{\Delta \alpha l}{4 \cos \theta} \right) \cos 2\Omega t. \quad (4)$$

For arbitrarily large phase modulations,  $\Delta$  and  $\Delta^2$  in equations (3) and (4) must be replaced by  $J_0(\Delta)J_1(\Delta)$  and  $J_0(\Delta)J_2(\Delta)$ , respectively, where  $J_{0,1,2}$  are Bessel functions of order 0, 1 and 2, respectively. Thus by measuring the fundamental and second harmonic signal from the lock-in we can determine the amplitude and phase of the absorption and refractive index gratings. In the derivation of equations (3) and (4) it was supposed that the material response of the internal space-charge field is harmonic, i.e. the electroabsorption and electrorefraction grating are copies of the intensity distribution. This is true under many operating conditions, so the results deduced from equations (3) and (4) are generally valid for quantum wells operated in the transverse or Franz–Keldish geometry.

Since  $\Delta \alpha$  and  $\Delta n$  are wavelength-dependent, tuning the wavelength of the interference beams around the excitonic peaks allows us to measure the spectra of the diffracted beam from both gratings. In summary, the advantage of this technique is that we can measure simultaneously both absorption and refractive index changes without relying on TWM measurements or complicated Kramers–Kronig numerical calculations.

Equations (3) and (4) are valid only when the modulation frequency  $\omega$  is much larger than the inverse of the space-charge field formation time ( $\tau$ ). In such a regime, the space-charge field is static as compared to the rapidly changing intensity pattern and therefore frequency independent. However, for low frequencies the space-charge field follows almost instantaneously the intensity changes, giving a small diffracted signal. The frequency dependence of the electroabsorption (hence diffracted signal, equation (3)) can be described by

$$\Delta n(\Omega) = \Delta n^\infty \frac{\Omega \tau}{1 + \Omega \tau} \quad (5)$$

where  $\Delta n^\infty$  is the value of the refractive index change at high frequency. If  $\Omega \ll \tau^{-1}$ , then the diffracted signal increases linearly with frequency. On the other hand, if  $\Omega \gg \tau^{-1}$  the diffracted signal is frequency-independent. Thus the response time of the electroabsorption can be obtained when  $\Omega = \tau^{-1}$ . Equation (5) represents a novel and simple way of measuring the response time of photorefractive gratings, as opposed to the traditional way of monitoring the temporal behaviour of the gratings [7]. A similar expression can be found for the absorption coefficient change.

## 3. Experiment

The experimental set-up is shown schematically in figure 1. A manually tunable diode laser (Newport Mod. 2010) was used to write the gratings. The laser tuning range (from 820

to 855 nm) conveniently covers the excitonic peaks. The sample consists of 100 periods of 10 Å GaAs wells and 60 Å Al<sub>0.3</sub>Ga<sub>0.7</sub>As barriers grown by molecular beam epitaxy at 600 °C on a semi-insulating substrate. The superlattice was proton-implanted after growth with two doses of  $1 \times 10^{12} \text{ cm}^{-2}$  at energies of 80 and 160 keV to make it semi-insulating. The quantum wells were grown on a stop-etch layer of 5000 Å of Al<sub>0.5</sub>Ga<sub>0.5</sub>As which permitted the samples to be epoxied to a glass slide and the substrate removed to perform optical transmission experiments. The total thickness of the device was  $\sim 1 \mu\text{m}$ . Titanium–gold electrodes were deposited on the free surface of the device. The laser beam was split into two beams of equal intensity ( $m = 1$ ) by means of a beamsplitter. The beams are made to interfere on the sample by using a couple of mirrors. The angle between beams was  $0.6^\circ$ , giving a grating spacing of 37  $\mu\text{m}$ . The reference beam is phase-modulated with amplitude  $\Delta$  and frequency  $\Omega$  by using a Pockel's cell phase modulator. A function generator drives the phase modulator and provides the reference signal for the lock-in amplifier. The modulated and reference beams interfere on the sample, creating an absorption and refractive index grating with varying amplitude, depending on the magnitude of the applied electric field. A *pin* photodetector from EOT Mod. ET-2030 with responsivity of  $0.4 \text{ A W}^{-1}$  at 830 nm placed after the sample measured the periodically diffracted signal. A 10 k $\Omega$  resistor was used as the load for the photodiode and the signal was sent to the lock-in amplifier Mod. SRS 530. A high voltage applied on 1 mm electrode separation provides electric fields of the range of 0–12 kV  $\text{cm}^{-1}$ . Under the above conditions, the quantum wells were operated in the Franz–Keldish geometry.

#### 4. Results and discussion

In order to find the excitonic peak's position and the magnitude of the change in absorption coefficient, differential transmission of the sample was measured under 8 kV  $\text{cm}^{-1}$  with a spectrophotometer. Differential absorption was calculated from  $\Delta\alpha = -\ln(1 + \Delta T/T)/l$ , where  $\Delta T$  is the differential transmission with field  $T(E_0)$  and without field  $T$  and  $l$  is the sample thickness ( $\sim 1 \mu\text{m}$ ). In this expression, Fabry–Perot effects were not taken into account. Changes in  $\Delta\alpha$  of  $400 \text{ cm}^{-1}$  are observed at  $\lambda \approx 831 \text{ nm}$  (full curve in figure 2). By reversing the polarity of the electric field a  $\sim 30\%$  decrease in the peak value of  $\Delta\alpha$  was observed. This feature is very common and shows the importance of good quality electrodes in order to obtain the absorption and refractive index gratings from TWM experiments. Also, the refractive index change spectra are shown in figure 2 (broken curve) obtained from the Kramers–Kronig relation. The largest  $\Delta n \approx 0.015$  is obtained at  $\lambda \approx 833 \text{ nm}$ .

The spectra of the absorption (○) and refractive index (■) changes calculated by using equations (3) and (4) are also shown in figure 2. A good agreement between dynamic holography and differential transmission measurements can be seen. Given the high sensitivity of PMTWM, the electroabsorption features are better resolved than electroabsorption obtained from differential transmission. The maximum output diffraction efficiency is  $\sim 1 \times 10^{-4}$  and  $3 \times 10^{-4}$  for the index and the absorption grating at

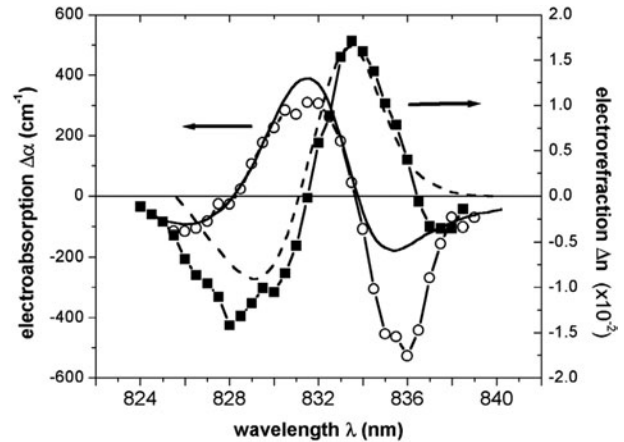


**Figure 2.** Electroabsorption (full curve) and electrorefraction (broken curve) spectra measured by differential transmission and calculated from the Kramers–Kronig relation. Measured electrorefraction (■) and electroabsorption (○) in GaAs quantum wells for  $E_0 = 8 \text{ kV cm}^{-1}$  from phase-modulated holography.  $\Lambda = 37 \mu\text{m}$ ,  $\Delta = 0.5 \text{ rad}$ ,  $\Omega/2\pi = 30 \text{ kHz}$ ,  $I_{\text{total}} = 6.1 \text{ mW cm}^{-2}$ . Lines in the experimental data are guides for the eye only.

8 kV  $\text{cm}^{-1}$ , respectively. These values agree well with reported values of the diffraction efficiency under similar conditions. Thus, PMTWM can be used to efficiently write and read the phase and refractive index gratings with their respective signs. Additionally, it is conveniently suited for low diffraction holograms since the diffracted signals are proportional to  $\Delta\alpha$  and  $\Delta n$  and not to  $\Delta\alpha^2$  and  $\Delta n^2$  (i.e. several orders of magnitude more sensitive), as occurs with diffraction efficiency experiments either in standard TWM or four-wave mixing techniques.

For applied fields larger than 3 kV  $\text{cm}^{-1}$ , refractive index gratings in PRMQW operating in the transverse configuration respond nonlocally to spatial varying optical illumination. For the field used in this paper a large phase shift is induced and therefore nonreciprocal energy transfer is possible. However, since PMTWM techniques do not rely on energy transfer, the information about the phase of the refractive index grating cannot be obtained. The phase of the nonlocal grating can be obtained by combining nonreciprocal energy transfer and four-wave mixing measurements [8]. Figure 3 shows the field dependence of electrorefraction at  $\lambda = 833 \text{ nm}$  and electroabsorption at  $\lambda = 831 \text{ nm}$ . Both curves show a quadratic dependence for low fields and eventually both saturate at the same field. Such a quadratic dependence is typical of the Franz–Keldish effect for semiconductors for energies below the bandgap [8].

Higher-order spatial harmonics can be generated in PRMQW when the modulation index approaches 1 [9]. In our experiment we observed first-order diffraction for the first, second and third harmonics gratings. The possibility of observing second- or higher-order diffractions can be ruled out because a maximum diffraction efficiency of  $10^{-8}$  for second-order diffraction is expected. First-order diffraction from the second harmonic grating is six times smaller than that from the first harmonic grating. Diffraction from the third harmonic is even smaller. Thus, the analysis described above remains valid with an uncertainty of 16%. However, the sensitivity of the technique can be dramatically increased by reducing

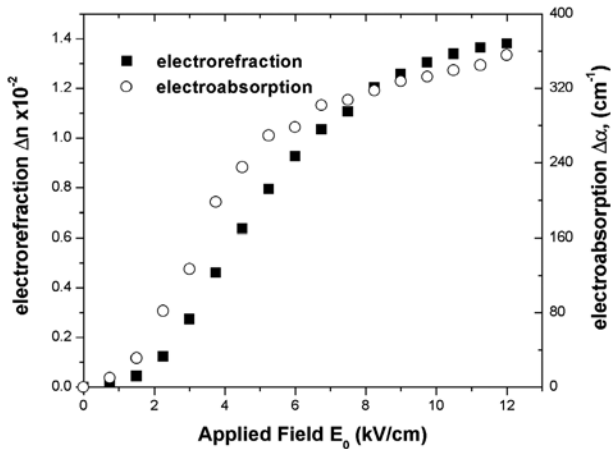


**Figure 3.** Field dependence of the electrorefraction and electroabsorption. Note that both curves scale quadratically for low fields and saturate at the same field.  $\Lambda = 37 \mu\text{m}$ ,  $\Delta = 0.5 \text{ rad}$ ,  $\Omega/2\pi = 30 \text{ kHz}$ ,  $I_{\text{total}} = 6.1 \text{ mW cm}^{-2}$ .

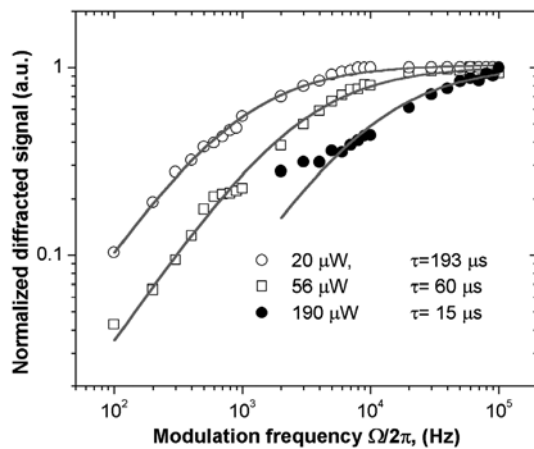


**Figure 4.** Frequency dependence of the diffracted signal for three different powers ( $\circ$ )  $20 \mu\text{W}$  ( $1.6 \text{ mW cm}^{-2}$ ), ( $\square$ )  $56 \mu\text{W}$  ( $3.2 \text{ mW cm}^{-2}$ ) and ( $\bullet$ )  $190 \mu\text{W}$  ( $11 \text{ mW cm}^{-2}$ ). Lines are fitted to equation (5), from where the response time of the grating formation is obtained.  $\Lambda \sim 37 \mu\text{m}$ ,  $E_0 = 8 \text{ kV cm}^{-1}$ ,  $\lambda = 833 \text{ nm}$ .

the modulation index, since diffraction from higher harmonics decreases rapidly ( $\sim m^4$  for second harmonic grating).

In order to maximize our signal one should use a modulation frequency much larger than the inverse of the dielectric relaxation time (or response time for grating formation) ( $\Omega \gg 1/\tau$ ) of the quantum well. The results presented above fulfilled this condition. Figure 4 shows the frequency dependence of the refractive index grating at the modulation frequency for three different intensity values. At low frequency, the diffracted signal scales linearly with frequency and is frequency-independent at high frequency. The lines are fitted to equation (5), from where the response time can be obtained. As the intensity increases, the response time decreases proportionally. For beam power as low as  $\sim 190 \mu\text{W}$  ( $\sim 11 \text{ mW cm}^{-2}$ ) a response time of  $15 \mu\text{s}$  is obtained, showing that PRMQW of GaAs are one of the most sensitive and fastest photorefractive materials. This result agrees with previous measurements of the response time of the grating by monitoring the time evolution [7].

The application of this technique can be extended to other areas where the study of the absorption and the optical resonance of materials are the main objective, such as recoil-induced spectroscopy [10] and electromagnetically induced gratings in cold atoms [11], to mention just two examples.

## 5. Conclusions

We have shown that phase-modulated holography can effectively be used for high sensitivity measurements of electroabsorption and electrorefraction with their respective phases. Electrorefraction and electroabsorption can be directly measured from the first and second harmonic signals of the lock-in amplifier. The sensitivity of the technique is several orders of magnitude smaller than conventional TWM or four-wave mixing techniques since the measured signal is proportional to  $\Delta\alpha$  and  $\Delta n$  and not to  $\Delta\alpha^2$  and  $\Delta n^2$ . Response times as small as  $15 \mu\text{s}$  were obtained at powers of  $190 \mu\text{W}$  in the frequency domain. The technique can be applied to spectroscopic techniques where optical resonances are of interest.

## Acknowledgment

This work was supported by CONACyT grant J-32231E.

## References

- [1] Nolte D D 1999 Semi-insulating semiconductor heterostructures: optoelectronic properties and applications *J. Appl. Phys.* **85** 6259
- [2] Miller D A B, Chemla D S, Damen T C, Gossard A C, Wiegmann W, Wood T H and Burrus A C 1985 Electric field dependence of optical absorption near the band gap of quantum-well structures *Phys. Rev. B* **32** 1043
- [3] Nolte D D, Olson D H, Doran G E, Knox W H and Glass A M 1990 Resonant photodiffractive effect in semi-insulating multiple quantum wells *J. Opt. Soc. Am. B* **7** 2217–25
- [4] Wang Q N, Nolte D D and Melloch M R 1991 Two-wave mixing in photorefractive AlGaAs–GaAs quantum wells *Appl. Phys. Lett.* **59** 256
- [5] Nolte D D, Chen N P, Melloch M R, Montemagno C and Haegel N M 1996 Electroabsorption field imaging between coplanar metal contacts on semi-insulating semiconductor epilayers *Appl. Phys. Lett.* **68** 72
- [6] Gehrtz M, Pinsl J and Brauchle C 1987 Sensitive detection of phase and absorption gratings: phase modulated homodyne detected holography *Appl. Phys. B* **43** 61
- [7] Balasubramanian S, Lahiri I, Ding Y, Melloch M R and Nolte D D 1999 Two-wave mixing dynamics and nonlinear hot-electron transport in transverse-geometry photorefractive quantum wells studied by moving grating *Appl. Phys. B* **68** 863
- [8] Wang Q, Brubaker R M, Nolte D D and Melloch M R 1992 Photorefractive quantum wells: transverse Franz–Keldish geometry *J. Opt. Soc. Am. B* **9** 1626
- [9] Wang Q, Nolte D D and Melloch M R 1991 Spatial-harmonic gratings at high modulation depths in photorefractive quantum wells *Opt. Lett.* **16** 1944
- [10] Fisher M C, Dudarev A M, Gutiérrez-Medina B and Raizen M G 2001 FM spectroscopy in recoil-induced resonances *J. Opt. B: Quantum Semiclass. Opt.* **3** 279–87
- [11] Mitsunaga M and Imoto N 1999 Observation of an electromagnetically induced grating in cold sodium atoms *Phys. Rev. A* **59** 4773